Design of High-Capacity Micropiles for 2,900-ft Long Caracas-La Guaira Viaduct

Jesús E. Gómez, Ph.D., P.E., D.GE, Antonio Martin Fossa, Ing.

ABSTRACT: The predicted collapse of the original concrete arch viaduct across the Tacagua Valley near Caracas, Venezuela, prompted the emergency design and construction of a replacement structure. The new bridge was to permit access to the capital city from the city of La Guaira, which hosts the main international airport and maritime port, and is also home to tens of thousands of daily commuters. The southern abutment of the original viaduct was built in the 1950s, over a pre-existing slide that encompassed a large portion of the adjacent hillside. Since 1985, movements of the hillside generated deformations of the viaduct, including uplift at the center of the span. The original viaduct ultimately collapsed in 2006 after a total uplift in the center of the span of approximately 51 inches, and before the design of the replacement bridge was completed.

The longer, new structure was designed to by-pass the unstable hillside, and thus required a total of 7 pilasters, up to 216 ft tall, founded at the bottom of the valley. The ground conditions, tight emergency construction schedule, and difficult access favored the use of high-capacity micropiles over more traditional foundation techniques. Nearly 500 micropiles were used for the foundation of the pilasters and the abutments. The micropiles were designed using the LRFD methodology for factored loads reaching 420 metric tons in compression, and over 200 metric tons in uplift. The use of micropiles allowed significant reduction of the foundation schedule. The entire structure was functional after only 16 months from the start of the foundation work.

INTRODUCTION

The Caracas-La Guaira highway in Venezuela was built in the early 1950s. It links the capital city of Caracas with the main international airport and maritime port in La Guaira. Because many inhabitants of La Guaira and adjacent coastal towns work in Caracas, the highway carries significant daily commuter traffic of roughly 50,000 vehicles.

The highway traverses very difficult terrain with steep hills and deep ravines, and includes three viaducts and two tunnels. The southernmost viaduct on the Caracas side, formally called Viaduct No. 1, is the subject of this paper. The location of the viaduct is depicted in Figure 1, together with some significant features of the terrain at the site.

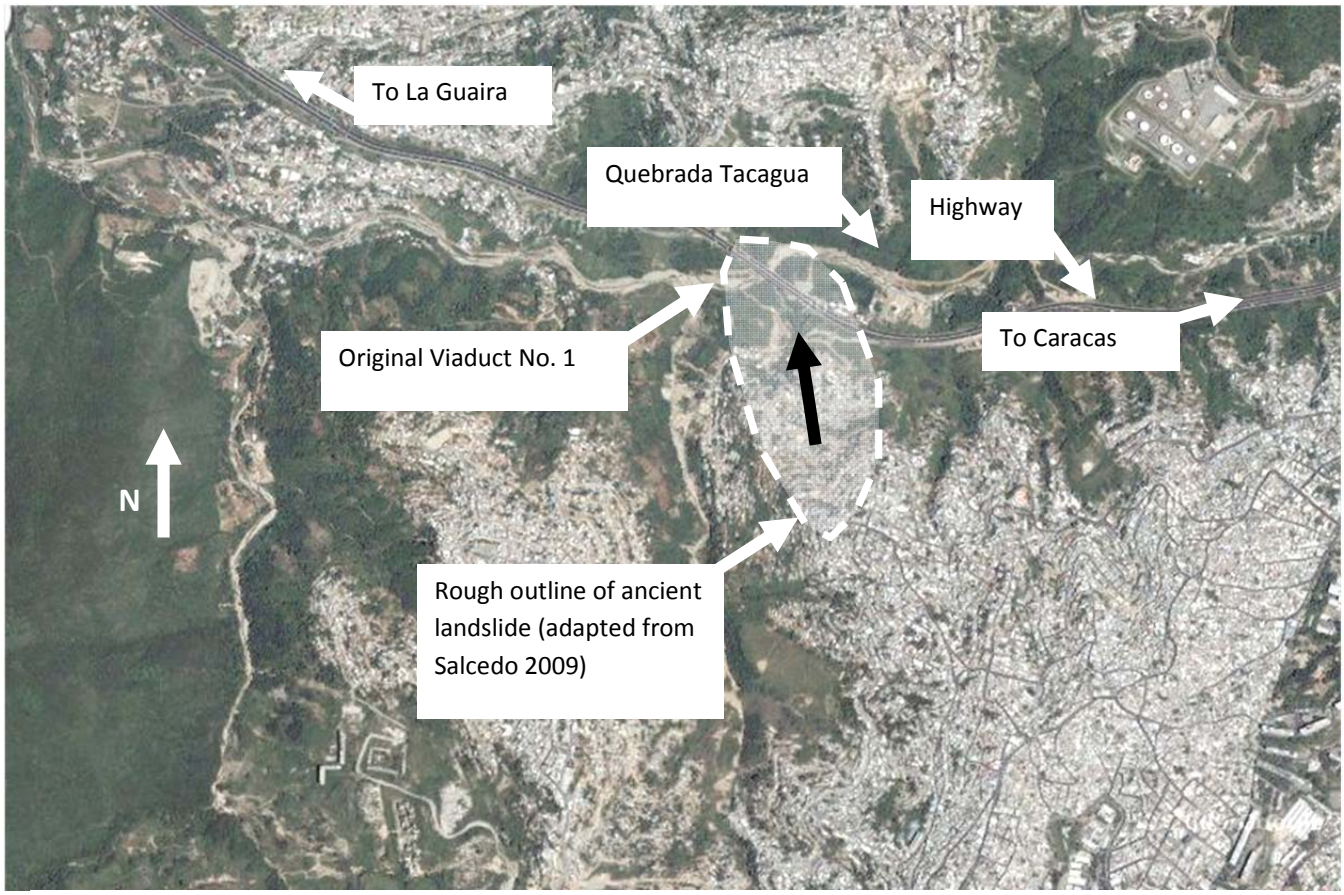

Figure 1. Location of Viaduct No. 1 and ancient slide (direction of thrust vector on viaduct is only approximate)

The viaduct collapsed in 2006 after significant deformations caused by a large landslide in the adjacent hillside. The viaduct was replaced by a longer structure bypassing the original landslide. This new structure was entirely supported on micropiles. The authors believe this may be the largest bridge entirely supported on micropiles in South America.

GEOLOGY AND SEISMICITY

According to the Venezuelan Foundation for Seismic Investigations (FUNVISIS 2002), most of the seismic activity in Venezuela is the product of the interaction between the Caribbean and the South American tectonic plates. The Fault Zone known as Falla de San Sebastián extends along the northern central Venezuelan coast and has been the source of some of the most destructive earthquakes in Venezuelan history.

Viaduct No. 1 crosses Quebrada Tacagua, a deep ravine with steep slopes which follows the trace of the geologically active Tacagua-Avila fault system. This fault zone has been singled out as causing significant earthquakes in central Venezuela and is the origin of abundant geotechnical problems along the southernmost portion of the Caracas-La Guaira highway.

Figure 2 is a typical section across Quebrada Tacagua (Carrillo 2007). Bedrock is a complex sequence of Graphite- and Mica- containing Schist, Calcareous Schist, Quartzite, Marble, and Amphibolites. The rock sequence is extensively folded and fractured with consistency varying

from soft to very hard. It is not uncommon to see very hard Quartzite intervals overlying softer and solutioned Calcareous Schist. Figure 3 is a view of an excavation at the site depicting the typical ground conditions.

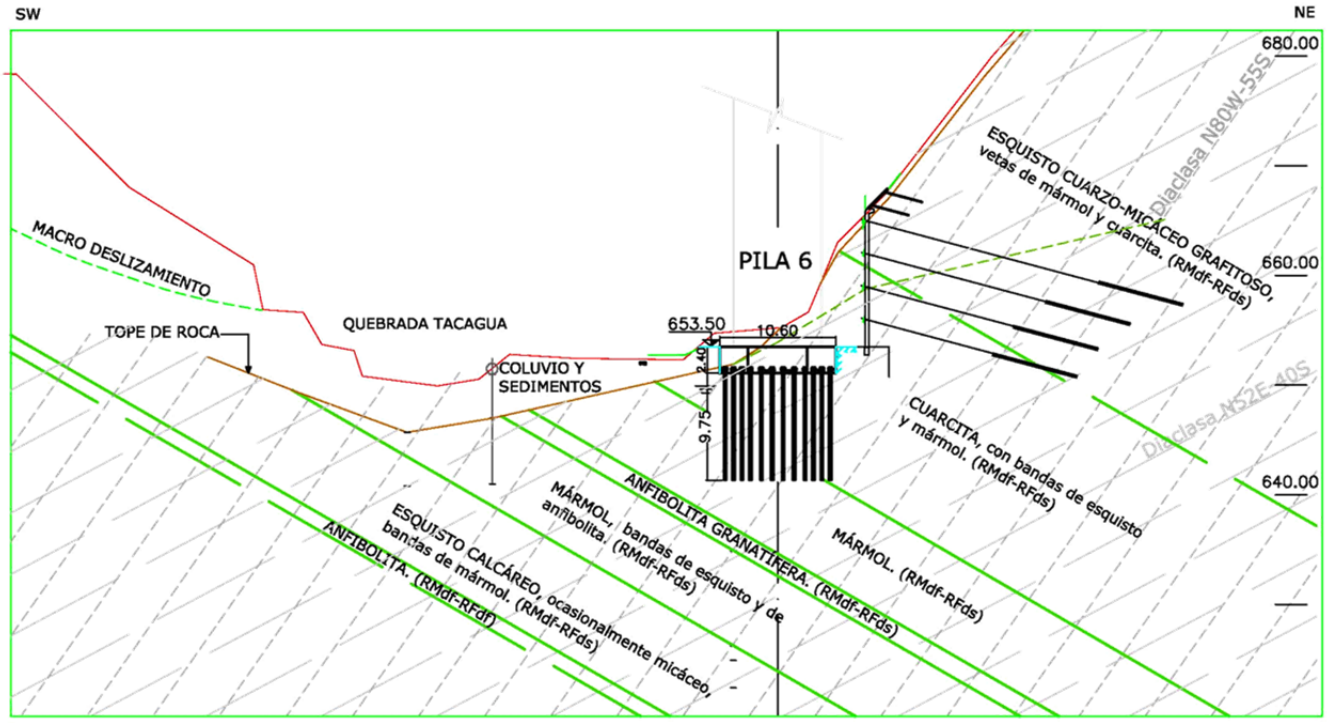

Figure 2. Typical cross-section through Quebrada Tacagua.

Figure 3. Ground conditions uncovered in an excavation for pilaster foundation.

PRE-EXISTING MASS MOVEMENT

Unbeknownst to its designers, the southern abutment and southern pilaster of the original Viaduct No. 1 were constructed on an ancient slide extending approximately 500 m (1650 ft), measured horizontally into the adjacent hillside, with a total elevation change of approximately 225 m (750 ft). The slide encompassed a total volume estimated in 6Mm^3 (8.2Myd^3). Salcedo (2009) provides a detailed description of the characteristics of the geology of the site, and the characteristics and history of the slide. Figure 1 depicts the approximate extent of the slide in relation to the original viaduct.

The movement rate of the slide was variable and ranged from 1 to 2 cm/year (0.4 to 0.8 in/year) in the 1990-1993 period, to roughly 2 to 20 cm/month (0.8 to 8 in/month) in 2005 (Salcedo 2009). Higher movement rates were measured before the collapse of Viaduct No. 1.

COLLAPSE OF ORIGINAL VIADUCT

The original viaduct was completed in 1952 and was opened to traffic in 1953. It had a total length of 308 m (1,020 ft). Figure 4 is a view of the viaduct soon after its construction. The structure of the bridge consisted of 3 parallel concrete arches spanning a total of 154 m (513 ft) with pilasters on each end. The deck was supported by prestressed girders along the entire length of the bridge. The southern pilaster was founded on hand-dug caissons. The southern abutment was founded directly on the ground.

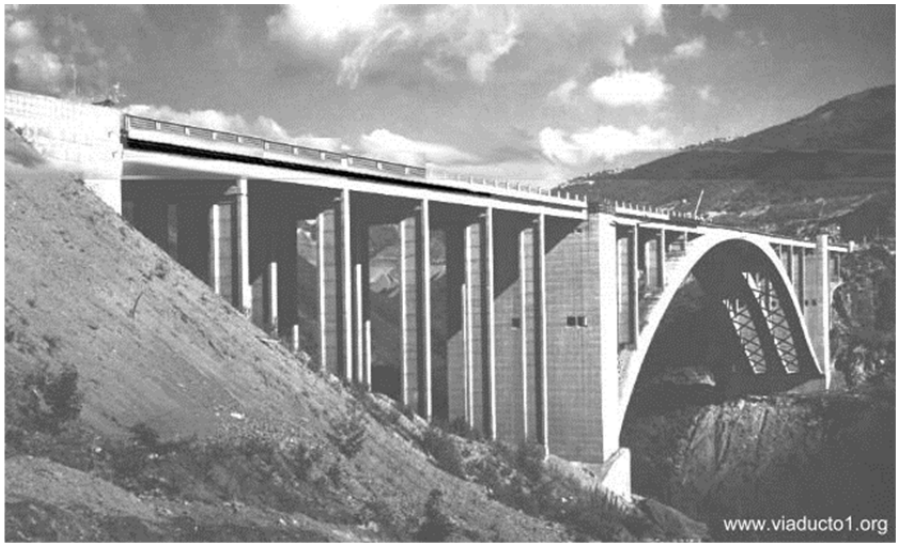

Figure 4. Original Viaduct shortly after its completion in 1952.

In 1987, heave of the pavement along the southern abutment was noticed. This prompted an intense structural and geotechnical investigation, which resulted in the discovery of the ancient slide and quantification of the rate of movement and prediction of its ultimate collapse. Various alternative solutions were proposed, which included, among others, the construction of a longer viaduct that would bypass the unstable area. However, a final mandate for the construction of a new viaduct was postponed due to the unstable political climate that has existed in the country since the 1980s.

In the meantime, engineering studies of the problem continued and temporary mitigation solutions were implemented that included installation of a large number of passive and active anchors through the unstable mass, release of internal structural stresses of the viaduct through controlled cutting of joints, and even installation of rollers or “skates” to allow movement of the bridge. These measures, in the opinion of the authors, did not do much to alleviate the problem and may have contributed to its acceleration.

As the displacement of the sliding mass continued, the bridge tended to compress. During this process, the mid-span point progressively rose until attaining a total upward vertical displacement of approximately 130 cm (51 in) shortly before its collapse.

The viaduct finally collapsed on March 19, 2006, two months after the viaduct had been shut down to vehicular and pedestrian traffic. During the time leading to the collapse, a temporary, alternate roadway winding to and from the bottom of the ravine had been constructed to permit vehicular traffic, which presented heavy congestion throughout the day. Figure 5 is a photo of the viaduct during its collapse snapped by a beachgoer. Figure 6 is a view after collapse of the viaduct.

Figure 5. Moment of collapse. Photo by A. Fonseca.

Figure 6. Viaduct after collapse.

NEW VIADUCT

The new viaduct is approximately 803 m (2,675 ft) long and bypasses the unstable landslide area that caused the collapse of the original viaduct. The structure is supported on seven “hammer head” pilasters reaching a maximum height of 61 m (203 ft) measured from the top of the foundation to the top of the pilaster and not including the 4-meter (13.1 ft) tall hammer head (Figures 7 and 8).

The pilasters have a hollow octagonal section with overall plan dimensions of 5 m by 8 m (16.67 ft by 26.67 ft). The span between pilasters is 110 m (366.67 ft). The deck is supported by three 500 cm (196.9 in) tall steel girders, which were launched from the northern abutment. The deck is composed of 25 cm (9 in) thick precast concrete slabs.

The design of the structure included a site-specific seismic analyses that yielded an acceleration coefficient of 0.43, site coefficient S=1, and seismic category D.

The factored loads at the base of the tallest pilaster used for the analysis of the various foundation alternatives were approximately 6,800 metric tons (15,000 kip) in axial compression load, and an overturning moment acting orthogonally to the axis of the bridge of up to 35,900 m-metric ton (259,000 ft-kip) primarily induced by seismic action.

The original design considered direct foundation of the pilasters on in situ rock. This required significant excavation through the highly variable rock formation to reach a suitable bearing stratum of sufficient thickness. At some pilasters, the excavation would have likely involved blasting through shallow layers of hard rock underlain by weaker strata that would generate significant settlement and even rotation of the pilasters.

Figure 7. Alignment of New Viaduct.

The foundation specialty contractor, Franki Foundations Venezuela, and its micropile consultant, Schnabel Engineering, proposed the use of micropiles as an economic foundation alternative. Although this technology was in use in the country at the time, it initially encountered significant resistance as the local engineers were not familiar with high-capacity micropile techniques.

Micropiles were ultimately selected for this project and were key to the success of the project from the perspective of schedule and cost. The typical foundation scheme is depicted in Figures 2 and 9. The main advantages of micropiles in this project were the following:

1. They were relatively easy to install in the difficult access conditions of the site
2. Large axial capacity of each micropile was achievable in the rock formation
3. Drilling of each micropile did not require re-tooling to traverse the various strata and could achieve a fast advancement rate
4. Micropiles could be load tested

5. Cost and schedule would be significantly reduced with respect to excavation and construction of a large reinforced concrete footing

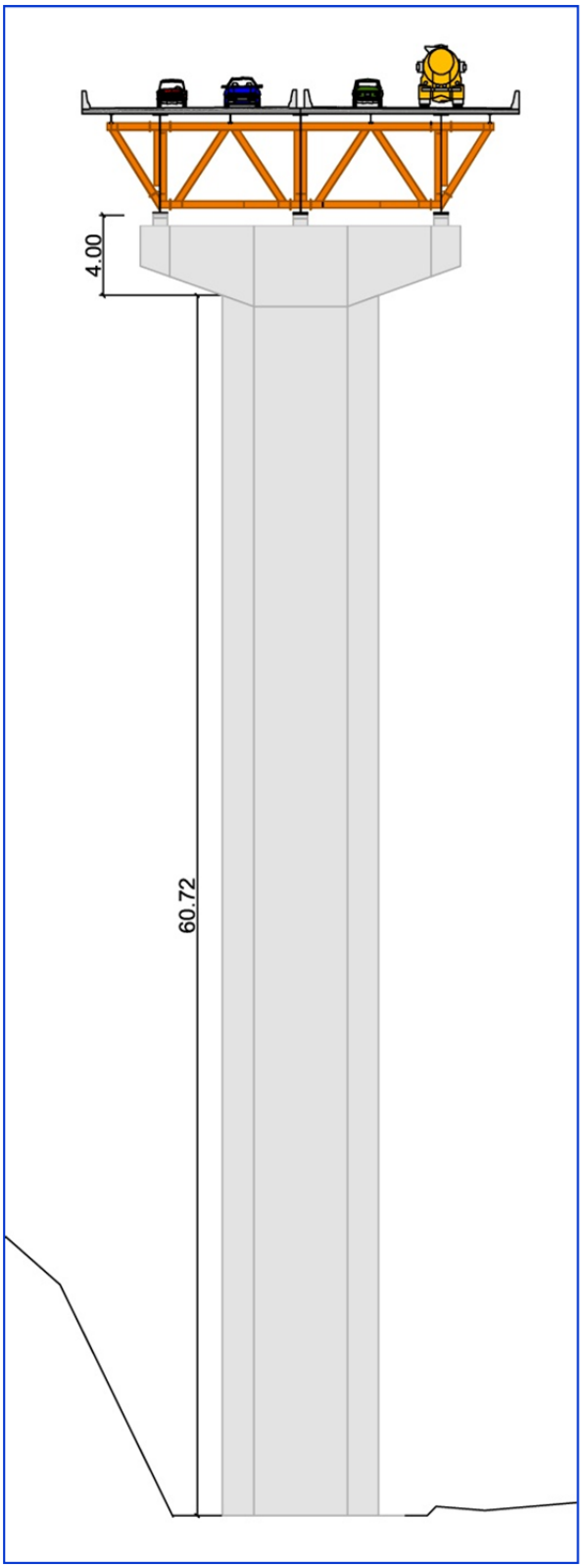

Figure 8. Typical pilaster.

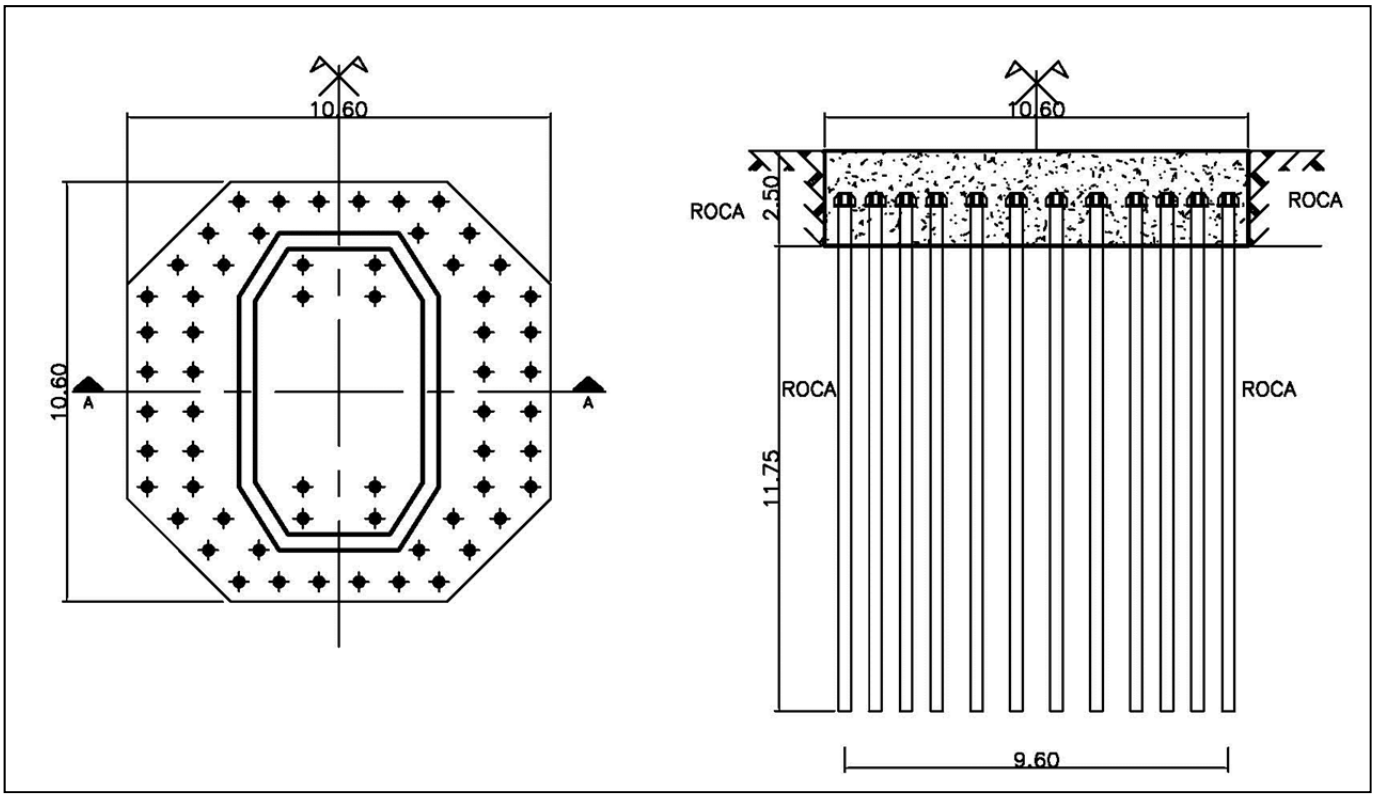

Figure 9. Foundation micropile arrangement. Dimensions are in meters (1 meter = 39.4 in).

DESIGN PROCESS

The pilaster foundations were designed using the Load and Resistance Factor Design (LRFD) approach. The critical design loads for the micropiles were obtained for the Extreme Event I load combination due to the significant seismic forces expected at the site. Strength I through V load combinations were not critical even though resistance factors that should be used for these combinations are lower than those for Extreme Event combinations.

The design followed an interesting sequence. Due to lack of suitable local sources of steel casing, the first step was to identify a supplier overseas and initiate procurement of the material. Franki Pile opted to import the micropile casing from Italy after careful consideration of cost and logistics. Because the micropiles were to be bonded into hard rock, it was decided in the initial stages of the design to use the largest casing available to maximize the structural capacity of the micropiles, and that could be practically installed within the limitations of the drilling equipment.

Once the casing was selected, the structural capacity of the micropile was calculated using LRFD. The structural engineer then followed an iterative process to establish an optimal micropile layout for each pilaster. The maximum and minimum reactions on individual micropiles of the group were determined using structural analysis computer software for each of the load combinations. The goal was to develop a micropile group with the minimum possible number of micropiles, and where the maximum and minimum micropile reactions did not exceed their structural resistance.

Geotechnical design of the micropiles was the last step in the design and consisted of establishing the bond length. Due to the fast track nature of the design process with frequent iterations required with the structural engineer, and due to the need to procure the casing with sufficient lead time, the bond length was defined so that the resulting geotechnical resistance exceeded the structural resistance of the micropiles.

STRUCTURAL AND GEOTECHNICAL RESISTANCE

The casing steel had a minimum Fy= 530 MPa (73 ksi). The casing had an external diameter of 177.8 mm (7 in), and a wall thickness of 20 mm (0.787 in). It provided most of the axial compression capacity and the entire axial tensile capacity; thus, a central bar was not required. The casing was installed in sections spliced by the use of an external threaded ring with cross sectional steel area slightly greater than the area of the casing steel. This type of connection is not typical in the United States, where flush male-female threaded connections are preferred because the permanent casing is often used as drill casing as well.

The nominal axial compression resistance of the micropile was approximately 390 metric tons (859 kip) as per AASHTO LRFD Bridge Design Specifications (AASHTO 2007). The nominal axial tensile resistance was approximately 252 metric tons (555 kip) in tension, which considered the reduction of tensile capacity due to the splice. This considered values of Resistance Factor of 0.75 and 0.8 in compression and tension, respectively. The calculation considered a corrosion thickness of 3 mm (0.12 in) around the casing.

It is interesting to note that the allowable axial compression load of the micropiles calculated following the Allowable Stress Design (ASD) approach was approximately 215 metric tons (477 kip). This value was used to verify the design against unfactored live and dead loads without lateral action of earthquake or wind, and to verify the maximum load to be applied to the test piles.

The geotechnical resistance was calculated using the lower end of the range of nominal grout-to-ground bond strength given by AASHTO (2007) for gravity-grouted micropiles in limestone. The value of α_b selected was 1,200 kPa (25 ksf).

To attain a nominal axial compression resistance of 390 metric tons (859 kip) or higher, and considering a 305 mm (12 in) grout body diameter, the minimum bond length was calculated as 4,900 mm (16 ft). This calculation considered a resistance factor of 0.7 as per AASHTO (2007), considering the performance of at least one load test per site condition. Final design considered a minimum micropile length of 10 meters (32 ft). This length was established based on examination of the geotechnical conditions and to achieve the minimum bond length into suitable limestone or harder rock in all micropiles.

MICROPILE INSTALLATION

The micropiles consisted of a permanent steel pipe installed in a predrilled hole. Drilling was accomplished by the use of a downhole hammer fitted with a button bit with nominal diameter

of 270 mm (10.625 in). Drilling was completed without significant problems at most locations and temporary casing or drilling fluid was not required for the most part.

Once drilling was complete, the hole was immediately filled with a neat cement grout mix. The primary quality control method for the grout was the specific gravity of the mix. The target specific gravity was set at a range of 1.8 to 1.9, which was verified using an API mud balance. In addition, grout cubes were also prepared and tested following requirements by the engineer. In the opinion of the authors, compressive testing of neat cement grout cubes is largely unwarranted as long as there is consistent cement and water chemistry.

Figure 10 shows the grout take volumes measured at one pilaster location. It is seen that the grout take was larger than theoretical due to the fracturing and open voids within the rock; however, the grout volumes were relatively consistent among micropiles.

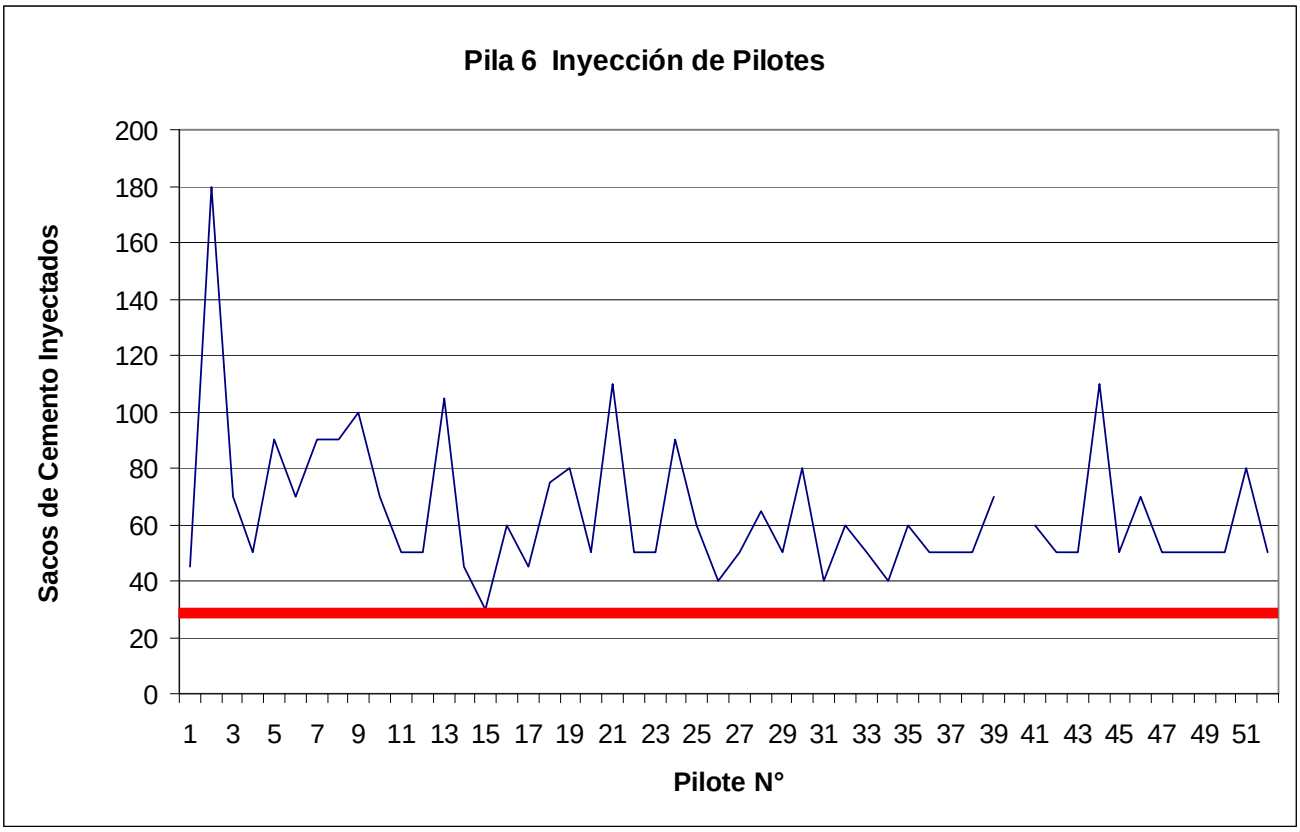

Figure 10. Grout take in bags of cement per micropile in Pilaster 6. Red line is the theoretical grout take.

Immediately after grouting of the hole, the reinforcing casing was installed into the fresh grout. Figures 11 and 12 show various features of the micropile materials and installation.

Figure 11. Casing used as micropile reinforcement.

Figure 12. Installation of casing in grout-filled hole.

The micropiles were connected to the pile cap through a special head designed by the structural engineer. This special head consisted of a short section of casing identical to the micropile casing that could be threaded to the top of the micropile. Thus, the casing of each micropile at the cutoff elevation was terminated with a threaded end and the splicing ring ready to receive the connection head. The head was fitted with a relatively thick plate and stiffeners as depicted in Figure 13, designed to withstand the design compression and tension forces.

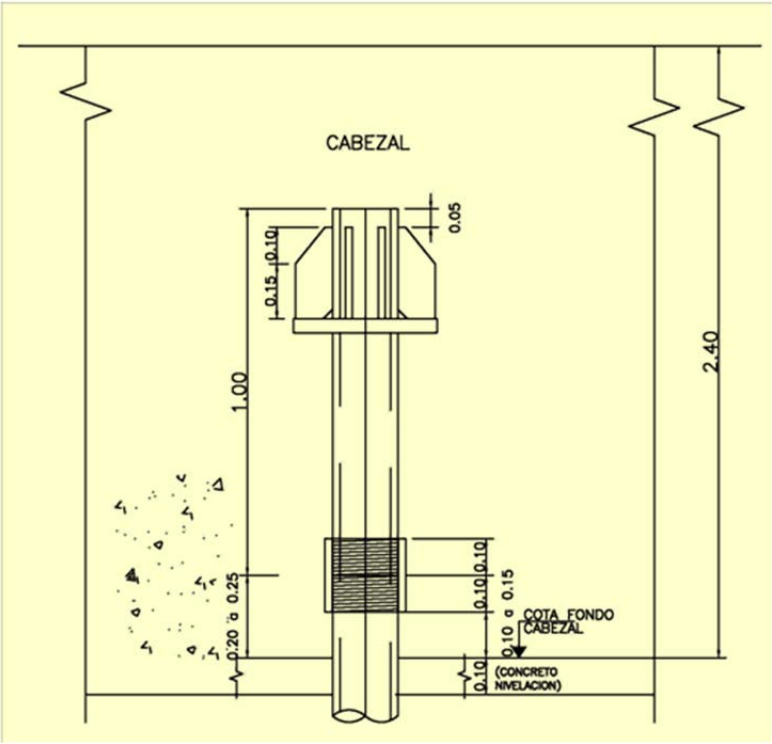

Figure 13. Micropile-cap connection detail (dimensions in meters).

This type of connection is not typically recommended for micropiles because of its cost, and because of the difficulties associated with welding and installation. In the United States, the preferred connection type is a single bearing plate affixed to the micropile by a central threadbar and a nut. The threadbar extends into the micropile a distance equal to at least the development length of the central bar. Welding is thus avoided.

The pile cap was a 10.6 m by 10.6 m by 2.4 m (34.8 ft by 34.8 ft by 7.9 ft) reinforced concrete cap as depicted in Figures 14 and 15.

Figure 14. View of pile cap construction.

Figure 15. Connection of micropile-to-pile cap.

LOAD TESTING

Three load tests in compression and in tension were performed across the length of the new viaduct at pilaster sites. The testing sites were selected based on the geotechnical conditions along the viaduct.

The load tests were carried to a maximum load of 430 metric tons (947 kip). This load was ten percent higher than the calculated nominal compression resistance of the micropiles and corresponded to twice the ASD-calculated allowable structural compression capacity of the micropile. None of the tests reached structural or geotechnical failure. The vertical deflection of the test micropiles ranged between 14 and 22 mm (0.55 and 0.87 in) under the maximum compression test load (see Figure 16).

VIADUCT CONSTRUCTION

Construction of pile caps, pilasters and upper structure closely followed the advancement of micropile installation as depicted in Figure 17. The structure advanced from the northern abutment, which was the launching site for the bridge girders. The pilasters were constructed using four hydraulic formwork systems that would permit continuous concrete pouring as the formwork slid vertically. The average rate of advancement was 200 mm/hour (8 in/hour). The verticality and twist of the formwork were controlled using lasers.

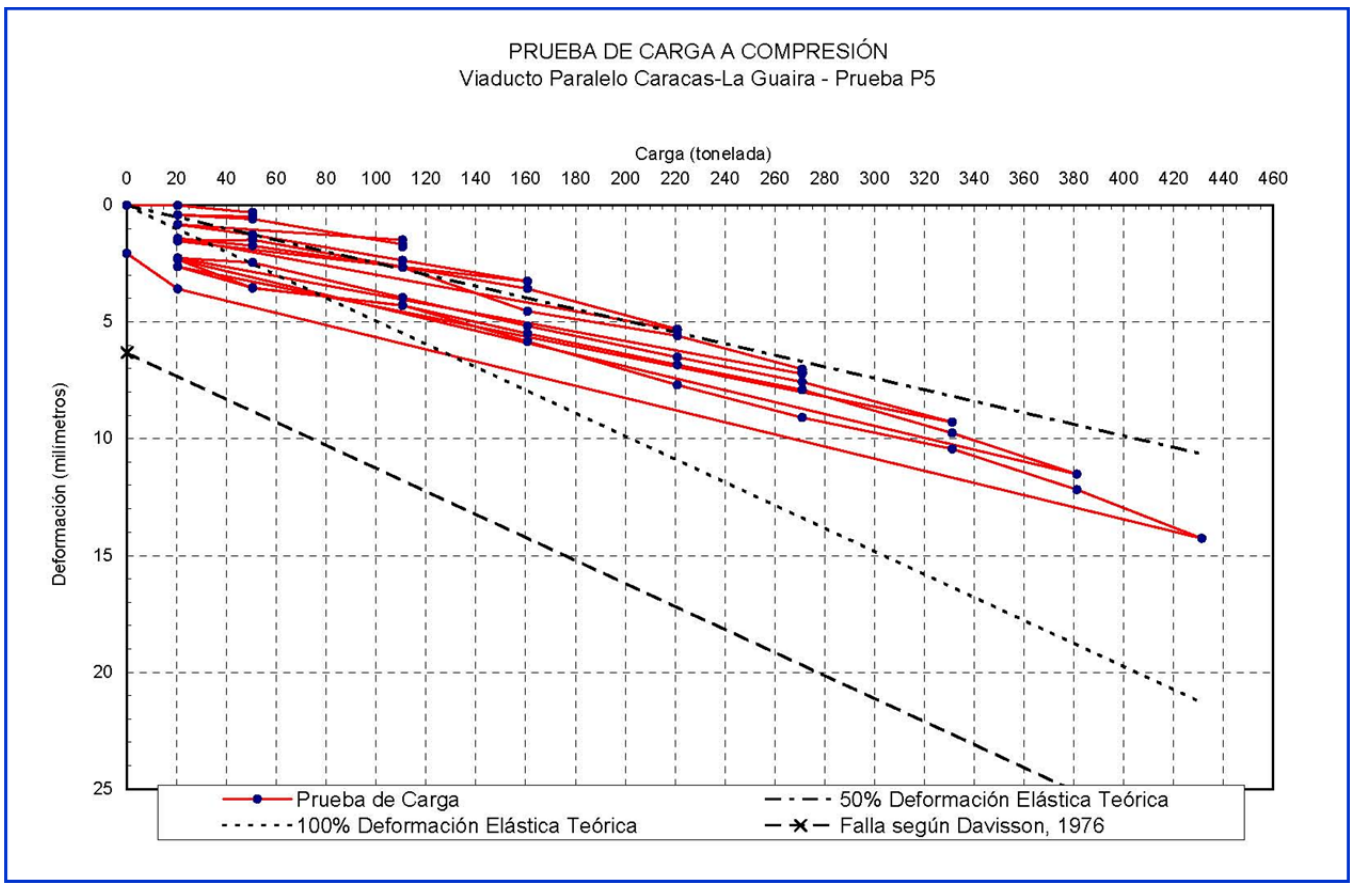

Figure 16. Results of one micropile load test at the site. Loads in metric tons and deflections in mm (1 metric ton = 2.2 kip, 25.4 mm = 1 inch).

Figure 17. Simultaneous foundation, pilaster, and girder installation.

The girders were built-up sections fabricated off site in the industrial city of Puerto Ordaz, and transported in 20 m (65.6 ft) segments via cargo ship to the Port of La Guaira, where they would be loaded on trucks for transport to the site. Once the initial girder segments were spliced and laced together at the fabrication shop on the southern abutment, they were fitted with a leading truss and launched using hydraulic jacks and rollers over special rails. Figure 18 depicts the launching process.

Figure 18. Launching girder.

The deck consisted of 704 precast concrete slabs, 11.2 m by 2.29 m (36.7 ft by 7.5 ft), with thickness ranging from 220 to 280 mm (8.66 to 11 in), which were placed using crawler cranes and attached using Nelson studs to the girder's top flange. The space between the slabs was backfilled with structural concrete.

Finally, a 5-cm (2-inch) thick surface course of asphalt concrete was placed over the deck. Figure 19 is a view of the completed structure. Construction took a total of 16 months since the start of foundation work, and the bridge was opened to traffic on June 21, 2007.

Figure 19. Completed Viaduct.

CLOSURE

This unique project represented a success in terms of savings in construction cost and schedule. The implementation of micropiles early in the design phase of the Viaduct allowed rapid completion of the foundation work. Micropile installation advanced at an accelerated pace and allowed significant savings in schedule. The total construction time since the start of site preparation was 16 months, which was 4 months shorter than the originally anticipated 20-month schedule. To a great extent, schedule savings were due to the utilization of micropiles.

The project was also a success in terms of the introduction of state-of-the-art micropile technology in Venezuela. This project gave impetus to the use of high-capacity micropiles throughout the country in residential and commercial construction.

ACKNOWLEDGEMENTS

The authors wish to acknowledge the contribution and help of Antonio Martin Fossa, Alain Boulanger, and Leonardo Quijada of Franki Pile Venezuela, as well as the significant resources provided by Schnabel Engineering for the completion of this paper.

REFERENCES

AASHTO (2007), “AASHTO LRFD Bridge Design Specifications, 4th Edition,” American Association of State Highway and Transportation Officials, Washington, DC.

Carrillo, P. (2007) personal communication.

FUNVISIS (2002), “La investigación sismológica en Venezuela,” Fundación Venezolana de Investigaciones Sismológicas, Impesos Lauper, Caracas, Venezuela. Available at http://www.funvisis.gob.ve/archivos/pdf/libros/funvisis_1_18.pdf.

Precomprimidos (2007), “Proyecto y construcción del Nuevo viaducto alterno Caracas La Guaira. Un reto a la ingeniería,” II Congreso Iberoamericano de Ingeniería Civil, Mérida, Venezuela, November 8, 2007.

Salcedo, D.A. (2009), “Behavior of a landslide prior to inducing a viaduct failure, Caracas-La Guaira highway, Venezuela, “ Engineering Geology, Volume 109, Issues 1-2, The Mechanics and Velocity of Large Landslides, 29 October 2009, Pages 16-30, ISSN 0013-7952, DOI: 10.1016/j.enggeo.2009.02.001. (http://www.sciencedirect.com/science/article/B6V63-4VNH43W-1/2/729b81b98a3ce30f809807613db5b584).